

Mutational and inhibitive analysis of SARS coronavirus 3C-like protease by fluorescence resonance energy transfer-based assays

Wan-Fen Kuang^a, Lu-Ping Chow^b, Mei-Hua Wu^a, Lih-Hwa Hwang^{a,*}

^a Hepatitis Research Center, National Taiwan University Hospital, National Taiwan University College of Medicine, Taipei, Taiwan, ROC

^b Graduate Institute of Biochemistry and Molecular Biology, National Taiwan University College of Medicine, Taipei, Taiwan, ROC

Received 10 April 2005

Available online 28 April 2005

Abstract

The 3C-like protease (3CL^{PRO}) of severe acute respiratory syndrome coronavirus (SARS-CoV) plays key roles in viral replication and is an attractive target for anti-SARS drug discovery. In this report, a fluorescence resonance energy transfer (FRET)-based method was developed to assess the proteolytic activity of SARS-CoV 3CL^{PRO}. Two internally quenched fluorogenic peptides, 1NC and 2NC, corresponding to the N-terminal and the C-terminal autocleavage sites of SARS-CoV 3CL^{PRO}, respectively, were used as substrates. SARS-CoV 3CL^{PRO} seemed to work more efficiently on 1NC than on 2NC in *trans*-cleavage assay. Mutational analysis demonstrated that the His41 residue, the N-terminal 7 amino acids, and the domain III of SARS-CoV 3CL^{PRO} were important for the enzymatic activity. Antibodies recognizing domain III could significantly inhibit the enzymatic activity of SARS-CoV 3CL^{PRO}. The effects of class-specific protease inhibitors on the *trans*-cleavage activity revealed that this enzyme worked more like a serine protease rather than the papain protease.

© 2005 Elsevier Inc. All rights reserved.

Keywords: SARS coronavirus; 3C-like protease; FRET-based proteolytic assay

Proteolytic processing of viral polyproteins is a key step in the replication cycle of many positive-stranded RNA viruses, and such processing in severe acute respiratory syndrome coronavirus (SARS-CoV) is performed by papain-like protease and 3C-like protease (3CL^{PRO}) [1]. The crystal structure of SARS-CoV 3CL^{PRO} was recently resolved by two groups [2,3], which reveal great similarity to the structure of the 3CL^{PRO} of porcine transmissible gastroenteritis virus (TGEV) and of human coronavirus (strain 229E), all of which form dimers [2,4]. Each monomer of the enzyme contains three structural domains: the first two domains form a chymotrypsin fold containing the catalytic site comprised of His41 and Cys145, and the third domain is a globular α -helical structure which is linked to domain II by a long loop

[2–4]. The extra helical domain III is unique for coronavirus 3CL^{PRO} because the picornavirus 3C proteases only contain the chymotrypsin fold, but have no extra domain [5–7]. The role of domain III in SARS-CoV 3CL^{PRO} is not quite clear but seems to be involved in dimer formation [3,4,8]. Due to its functional importance, SARS-CoV 3CL^{PRO} becomes an attractive target for structure-based drug designs against SARS [9–12].

To fulfill the needs of efficient and robust high-throughput screening of the anti-protease drugs, a convenient assay system for measuring the enzymatic activity is needed. In this study, we have established a fluorescence resonance energy transfer (FRET)-based method to assess the proteolytic activity of SARS-3CL^{PRO}. Two internally quenched fluorogenic (IQF) 11-mer peptides with N-terminus conjugated with an *ortho*-aminobenzoic acid (Abz) and C-terminus conjugated with a lysine-2,4-dinitrophenylamide (Lys-DNP) were synthesized and used as substrates. Upon cleavage of the substrate, the

* Corresponding author. Fax: +886 2 23825962.

E-mail address: lihwa@ha.mc.ntu.edu.tw (L.-H. Hwang).

fluorophore was separated from the quenching group, generating a fluorescence signal [13,14]. The enzymatic reactions were monitored in real time. Using the FRET-based method, we have characterized the enzymatic activities of a catalytic site-mutated 3CL^{pro} (H41A), a N-terminus-deleted 3CL^{pro} (Δ 1–7), and a domain III-deleted 3CL^{pro} (Δ III). We also used the system to demonstrate that some protease inhibitors and monoclonal antibodies recognizing domain III had inhibitory effects on the proteolytic activity of SARS-3CL^{pro}. The FRET-based real time assay provides an ideal platform for exploring the inhibitors against SARS-CoV 3CL^{pro} and is a convenient system to study the kinetics of proteolytic reactions.

Materials and methods

Construction of pET28b-3CL^{pro}. The cDNA corresponding to SARS-CoV (strain TW1) nt 9985–10,902 coding for the 3CL^{pro} protein was amplified by PCR from the reverse transcriptional mixture provided by Dr. P.J. Chen (Graduate Institute of Clinical Medicine, National Taiwan University, Taipei, Taiwan). The PCR product was cloned into the pET28b vector (Novagen) and the resulting plasmid, designated as pET28b-3CL^{pro}, was verified by sequencing.

Expression and purification of the 3CL^{pro} protein. The plasmid transformed *Escherichia coli* cells were grown at 37 °C until A_{600} reached 0.6–0.8 and then induced to express the recombinant protein with 0.5 mM isopropyl-1-thio- β -D-galactopyranoside (IPTG) for 3 h. The cells harvested were disrupted in buffer A (20 mM Tris–HCl, pH 8.0, 500 mM NaCl, and 5 mM imidazole) and cell lysate was applied to a nickel affinity column (Amersham Pharmacia Biotech AB, Uppsala, Sweden). After wash, the 3CL^{pro} protein was eluted with a 12–100% linear gradient of buffer B (20 mM Tris–HCl, pH 8.0, 500 mM NaCl, and 250 mM imidazole) in buffer A. The fractions containing 3CL^{pro} were pooled and dialyzed against the storage buffer (20 mM Tris–HCl, pH 8.0, 50 mM NaCl, and 1 mM EDTA). The sample was concentrated and stored at –80 °C in storage buffer containing 50% glycerol. The proteins were more than 95% pure as assessed by SDS–PAGE.

Deletion and point mutation. Using pET28b-3CL^{pro} as a template, three mutant clones (H41A, Δ 1–7, and Δ III) were generated by one-primer PCR method as described previously [15]. The single primer 5'-CACAGTATACTGTCCAAGAGCTGTCATTTGCACAGCAG-3' was used for the substitution of His41 with an alanine, primer 5'-CAGCAAATGGGTCGGGATCCCTTCCCGTCAGGCAAAGTTGAA-3' was used for the deletion of the N-terminal 1–7 amino acids of 3CL^{pro}, and primer 5'-GCAGGTACAGACACAACCATAGCGGCCGACTCGAGCACACCAC-3' was used for the deletion of the C-terminal 201–306 amino acids of 3CL^{pro}. All the mutant clones were verified by sequencing.

Protease activity assay using the IQF peptide substrates. Two synthetic IQF peptides, 1NC (Abz-Thr-Ser-Ala-Val-Leu-Gln↓Ser-Gly-Phe-Arg-Lys-DNP) and 2NC (Abz-Ser-Gly-Val-Thr-Phe-Gln↓Gly-Lys-Phe-Lys-Lys-DNP) (Genemed Synthesis, South San Francisco, CA), were used in this study (↓ indicates the cleavage site). The reaction mixture (30 μ l) contained 5 mM HEPES, pH 7.3, 1 mM DTT, 25 mM NaCl, 0.025% Triton X-100, 100 μ M peptide substrate, and 6 μ M 3CL^{pro}. Reactions were performed in a 384-well black microtiter plate incubated at 32 °C. After the enzyme was added, the increase of fluorescence was recorded continuously using a Labsystems fluorometer (Fluoroskan Ascent) with a plate reader accessory with excitation and emission wavelengths of 320 and 420 nm, respectively. The kinetic parameters were determined by Lineweaver–Burk plot using 6 μ M enzyme and 25–400 μ M peptide substrates.

Analysis of peptide cleavage by HPLC. The cleavage assays were carried out in a reaction mixture as described above for 3 h at 32 °C and then stopped by the addition of 1% formic acid. The reaction products were resolved on a C₁₈ analytic column (4.6 mm \times 250 mm, Beckman, Fullerton, CA) using a 0–60% linear gradient of 80% acetonitrile in 0.06% trifluoroacetic acid, at 1 ml min⁻¹ flow rate. The elution was monitored at an absorbance wavelength of 220 nm.

Inhibition assays. The inhibitory activities of protease inhibitors or antibodies toward 3CL^{pro} were measured in a reaction mixture lacking DTT in the presence of various concentrations (0–400 μ M) of the inhibitors or different amounts (0–5 μ l) of antiserum or monoclonal antibody ascites. Two cysteine protease inhibitors, *N*-ethylmaleimide (NEM) and E-64, and two serine protease inhibitors, *N* α -*p*-Tosyl-L-lysine chloromethyl ketone (TLCK) and *N*-*p*-Tosyl-L-phenylalanine chloromethyl ketone (TPCK) (Sigma), were used in this study. The antibodies used were rabbit anti-SARS-CoV 3CL^{pro} antiserum and three mouse anti-3CL^{pro} monoclonal antibodies (our unpublished data).

Results and discussion

Expression and purification of SARS-CoV 3CL^{pro} and its mutants

To establish a FRET-based assay, the wild-type SARS-CoV 3CL^{pro} was first expressed in *E. coli* and purified to nearly homogeneity (Fig. 1A). Meanwhile, three mutant proteins, the 3CL^{pro} having the His41 substituted with an Ala (H41A), a deletion of the N-terminal 1–7 amino acid residues (Δ 1–7), and a deletion of domain III (from aa 201 to 306) (Δ III), were expressed as well to assess the roles of the residue and the domains in the proteolytic activity of SARS-CoV 3CL^{pro}. Due to the extra sequences derived from pET28b, the full-length SARS-CoV 3CL^{pro} was expressed as a 39.5 kDa protein containing His₆-tag at both the N-terminus and the C-terminus. However, it was realized that the C-terminal sequences of SARS-CoV 3CL^{pro}, VTFQ, while in connection with the 11 amino acid residues of vector pET28b, AAALHHHHHH, could actually form a consensus cutting site for SARS-CoV 3CL^{pro}, VTFQ↓AAA. The resulting protein would then be

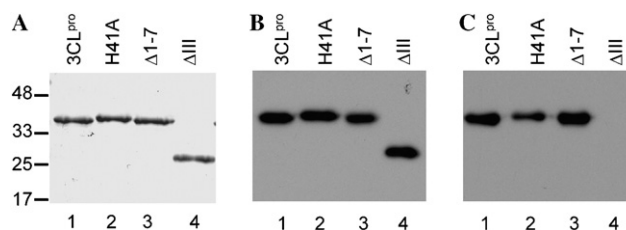


Fig. 1. Expression and purification of recombinant SARS-CoV 3CL^{pro} and its mutants. The recombinant proteins purified by Ni-affinity column were analyzed by SDS–PAGE on a 15% polyacrylamide gel and stained with Coomassie brilliant blue (A), or reacted with rabbit anti-SARS-CoV 3CL^{pro} polyclonal antiserum (B), or with a mouse monoclonal antibody, mAb 4, against SARS-CoV 3CL^{pro} (C). Molecular size markers (in kDa) are indicated on the left.

37.4 kDa instead of 39.5 kDa (Fig. 1A). Thus, the results clearly suggest that the SARS-CoV 3CL^{pro} expressed possesses *cis*-cleavage activity.

On the contrary, all the other three mutant proteins apparently did not possess proteolytic activities, their sizes were the same as anticipated, i.e., 39.5 kDa (H41A), 38.7 kDa (Δ 1–7), and 27.7 kDa (Δ III). All the 3CL^{pro} and mutant proteins were recognized by a rabbit anti-SARS-CoV 3CL^{pro} antiserum (Fig. 1B). However, all but Δ III were recognized by a mouse anti-SARS-CoV 3CL^{pro} monoclonal antibody (mAb 4) (Fig. 1C), suggesting that this monoclonal antibody might recognize the epitope residing in domain III.

Enzymatic activity of SARS-CoV 3CL^{pro} and its mutants

Two IQF peptides, 1NC and 2NC, were used for *in vitro trans*-cleavage assay. The sequences of these correspond to the N-terminal and the C-terminal autocleavage sites of SARS-CoV 3CL^{pro}, respectively. The enzymatic activities of SARS-CoV 3CL^{pro} toward

1NC and 2NC were analyzed by direct monitoring of the increase of fluorescence in real time (Fig. 2A). In parallel, the cleaved products obtained at the 3-h reaction were analyzed by reverse-phase HPLC (Fig. 2B). Both FRET-based and HPLC-based assays indicated that the wild-type SARS-CoV 3CL^{pro} had better cleavage efficiency on 1NC than on 2NC. According to the HPLC data, more than 90% of 1NC were cleaved by SARS-CoV 3CL^{pro} in 3 h, whereas only about 50% of 2NC were cleaved (Fig. 2B). Kinetic parameters were calculated based on the FRET-based assays. The K_m value for 1NC was 145.69 μ M, the K_{cat} was 0.604 min^{-1} , and the K_{cat}/K_m was 4.143 $\text{mM}^{-1} \text{min}^{-1}$. For 2NC, the K_m was 252.47 μ M, the K_{cat} was 0.303 min^{-1} , and the K_{cat}/K_m was 1.20 $\text{mM}^{-1} \text{min}^{-1}$.

On the contrary, the three mutants had extremely low proteolytic activities on both peptide substrates, as measured by FRET-based assays (Fig. 2A). The results indicate that the N-terminal 7 amino acids and the domain III are as important as the catalytic His41 residue in the proteolytic activity of SARS-CoV 3CL^{pro}.

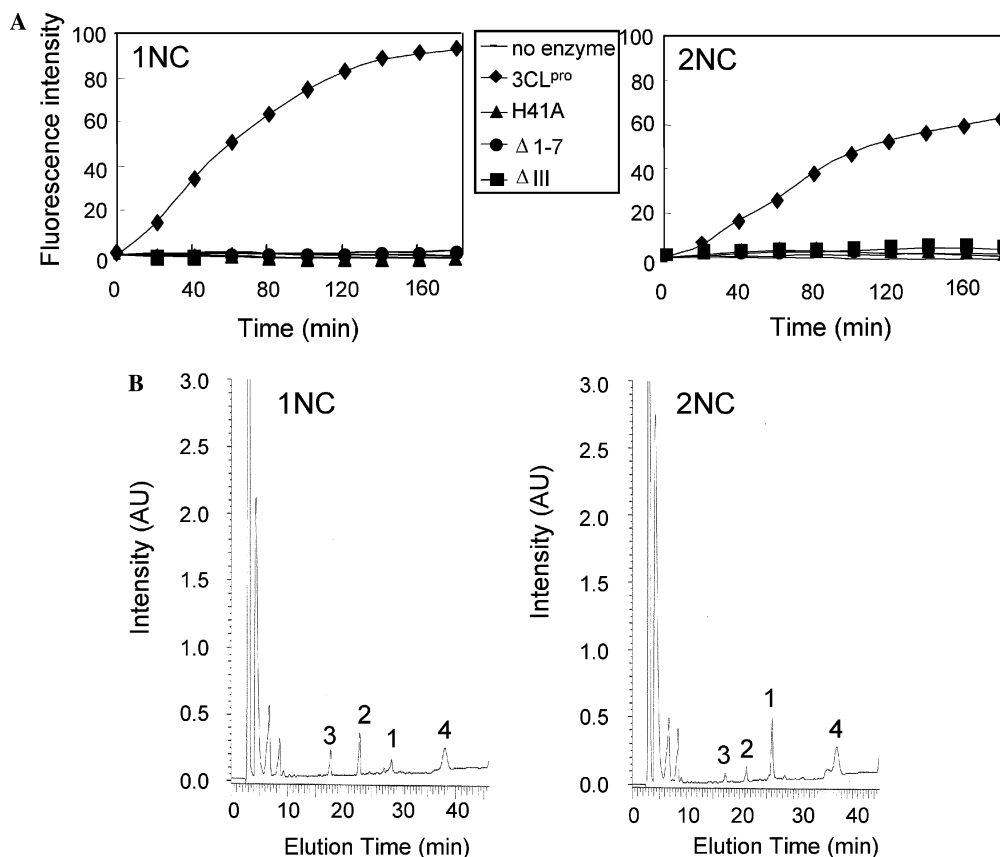


Fig. 2. Protease activity assays. (A) FRET-based method. The reaction contained 100 μ M IQF substrate (1NC or 2NC) and 6 μ M the wild-type SARS-CoV 3CL^{pro} or the mutant proteins, and carried out for 3 h as described under Materials and methods. The fluorescence was monitored in real time by a plate reader. (B) HPLC-based method. The reaction was carried out for 3 h and the cleaved products were analyzed by HPLC as described under Materials and methods. Peak 1 are the original peptide. Peaks 2 and 3 are the cleaved N-terminal and C-terminal fragments, respectively. Peak 4 are impurities in the original substrate solution.

Inhibitory effects of protease inhibitors on SARS-CoV 3CL^{pro}

SARS-CoV 3CL^{pro} belongs to the cysteine protease family with a chymotrypsin fold, thus it is interesting to know whether it is inhibited by serine protease inhibitors or by cysteine protease inhibitors. The inhibitory effects of two serine protease inhibitors, TLCK and TPCK, and two cysteine protease inhibitors, NEM and E-64, were tested in this FRET-based assay. Data shown in Fig. 3 demonstrate that both serine protease inhibitors reduced the enzymatic activity of SARS-CoV 3CL^{pro} in a dose-dependent manner. However, the results for the two cysteine protease inhibitors were inconsistent: while NEM had significant inhibitory effects on SARS-CoV 3CL^{pro}, E-64 did not inhibit it at all. The data support the idea that SARS-CoV 3CL^{pro} works following a general base mechanism like the serine proteases, but not following a thiolate–imidazolium ion pair catalytic mechanism like the papain protease [16]. However, NEM probably inhibits the proteolytic activity of SARS-CoV 3CL^{pro} via directly blocking the catalytic Cys145 residue, due to its ability to bind stoichiometrically to the sulfhydryl (SH) group of cysteine in the cysteine protease family.

Inhibition of SARS-CoV 3CL^{pro} activity by monoclonal antibodies that recognized domain III

Previously we have generated three monoclonal antibodies, mAb 3, mAb 4, and mAb 6, that could recognize full-length SARS-CoV 3CL^{pro} but not the protein lacking domain III (Fig. 1C and data not shown). We interpreted that these monoclonal antibodies probably recognized the epitopes residing in domain III. Therefore, we were interested to test whether they could inhibit the proteolytic activity of SARS-CoV 3CL^{pro} in the *trans*-cleavage assay. A rabbit anti-SARS-CoV 3CL^{pro} polyclonal antiserum was also tested. Data shown in Fig. 4 reveal that all three monoclonal antibodies could inhibit the enzymatic activity, whereas the polyclonal antiserum did not have the inhibitory activity. To our knowledge, this is the first report demonstrating that the enzymatic activity of SARS-CoV 3CL^{pro} could be inhibited by antibodies. The results further confirmed the pivotal roles of domain III in the proteolytic activity of SARS-CoV 3CL^{pro}.

In summary, a FRET-based method for detecting the proteolytic activity of SARS-CoV 3CL^{pro} was evaluated in this study. The kinetic studies showed that the N-terminal autocleavage site of SARS-CoV 3CL^{pro} was a better substrate than the C-terminal autocleavage site in the

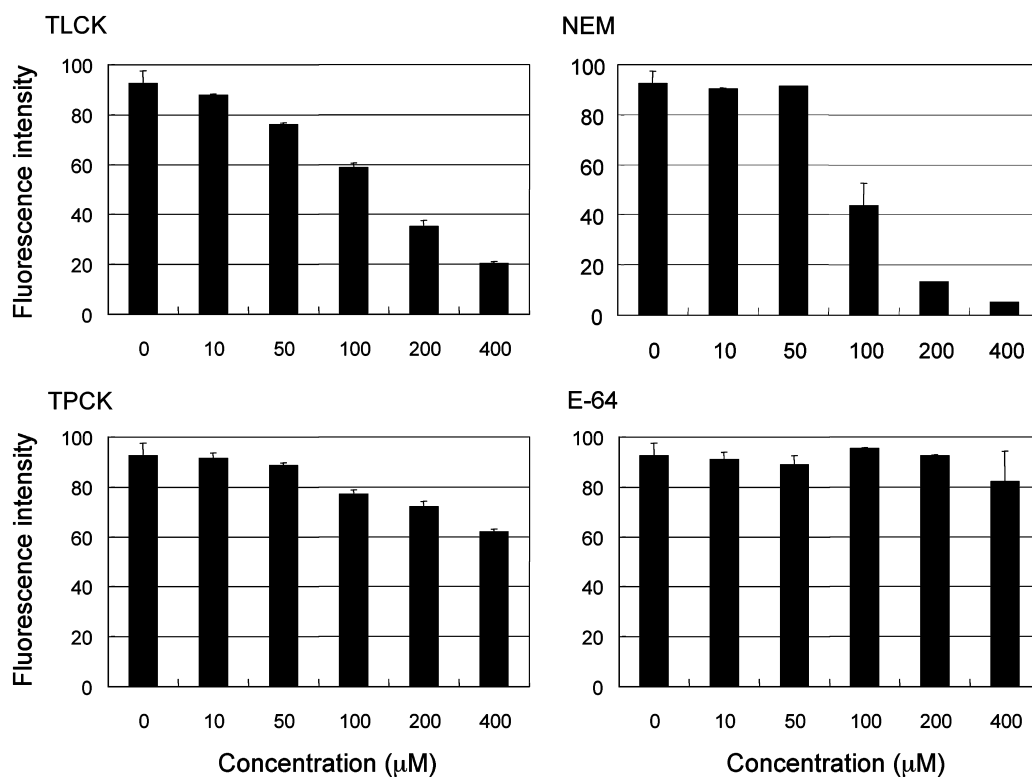


Fig. 3. Effects of protease inhibitors on the activity of SARS-CoV 3CL^{pro}. Two serine protease inhibitors, TLCK and TPCK, and two cysteine protease inhibitors, NEM and E-64, ranging from 0 to 400 μM were added to the reaction mixture containing the 1NC substrate. Fluorescence was monitored continuously. The data shown are the (means ± SD) fluorescence intensity at the 3-h reaction.

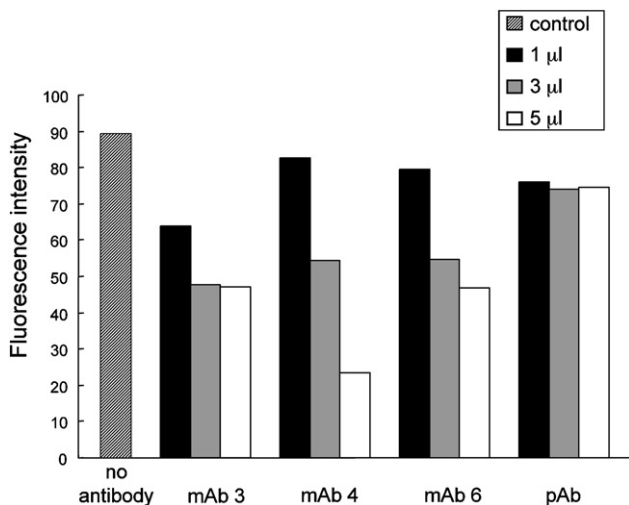


Fig. 4. Effects of antibodies on the activity of SARS-CoV 3CL^{pro}. Different amounts (1–5 μ l) of mouse anti-SARS-CoV 3CL^{pro} monoclonal antibody (mAb 3, mAb 4, or mAb 6) or rabbit anti-SARS-CoV 3CL^{pro} polyclonal antiserum (pAb) were added to the proteolytic reaction mixture containing the 1NC substrate and the fluorescence was monitored continuously. The data shown are the fluorescence intensity at the 3-h reaction.

trans-cleavage assay. Recently, Fan et al. [17] have systematically analyzed the substrate specificity of SARS-CoV 3CL^{pro} and found that the P2 position of the substrate required a large hydrophobic residue for the hydrophobic interaction between the P2 position and the S2 pocket of the enzyme, as indicated by the crystal structure [2,4]. Although Phe, Val, and Met are tolerant at P2 for SARS-CoV 3CL^{pro} [18], the mutation of Leu-P2 to other hydrophobic residues decreases the reaction activity [17]. Since 1NC has a Leu at the P2 position and 2NC has a Phe, this may explain why 2NC was cleaved less efficiently than 1NC by SARS-CoV 3CL^{pro}.

Our deletion data (Fig. 2) and antibody blocking data (Fig. 4) indicate that both the N-terminal 7 amino acids and the domain III are important for the enzymatic activity of SARS-CoV 3CL^{pro}. Similar conclusion has also been reached for the 3CL^{pro} of TGEV [4]. Previous crystal structure data have attributed this importance to the dimerization function mediated by these two domains [3,4,8,12]. However, a recent study by Chen et al. reported that the N-terminal seven amino acids of SARS-CoV 3CL^{pro} were not required for enzyme dimerization. Instead, they proposed that the N-terminus-deleted mutant had a conformation that reduced the size of the binding pocket, thus creating unfavorable conditions for substrate binding [19]. The discrepancy about the roles of the N-terminal seven amino acid residues is not completely resolved at this moment and it needs to be further investigated by different analytical methods. However, no matter what function the N-terminal domain may play, it is definitely important for the proteolytic activity of SARS-CoV 3CL^{pro}, as demonstrated by our activity assay.

Acknowledgment

This work was supported by Grant NSC 92-2751-B-002-004-Y from National Science Council of the Republic of China.

References

- [1] V. Thiel, K.A. Ivanov, A. Putics, T. Hertzog, B. Schelle, S. Bayer, B. Weissbrich, E.J. Snijder, H. Rabenau, H.W. Doerr, A.E. Gorbalenya, J. Ziebuhr, Mechanisms and enzymes involved in SARS coronavirus genome expression, *J. Gen. Virol.* 84 (2003) 2305–2315.
- [2] K. Anand, J. Ziebuhr, P. Wadhvani, J.R. Mesters, R. Hilgenfeld, Coronavirus main proteinase (3CL^{pro}) structure: basis for design of anti-SARS drugs, *Science* 300 (2003) 1763–1767.
- [3] H. Yang, M. Yang, Y. Ding, Y. Liu, Z. Lou, Z. Zhou, L. Sun, L. Mo, S. Ye, H. Pang, G.F. Gao, K. Anand, M. Bartlam, R. Hilgenfeld, Z. Rao, The crystal structures of severe acute respiratory syndrome virus main protease and its complex with an inhibitor, *Proc. Natl. Acad. Sci. USA* 100 (2003) 13190–13195.
- [4] K. Anand, G.J. Palm, J.R. Mesters, S.G. Siddell, J. Ziebuhr, R. Hilgenfeld, Structure of coronavirus main proteinase reveals combination of a chymotrypsin fold with an extra alpha-helical domain, *EMBO J.* 21 (2002) 3213–3224.
- [5] E.M. Bergmann, S.C. Mosimann, M.M. Chernaia, B.A. Malcolm, M.N. James, The refined crystal structure of the 3C gene product from hepatitis A virus: specific proteinase activity and RNA recognition, *J. Virol.* 71 (1997) 2436–2448.
- [6] D.A. Matthews, W.W. Smith, R.A. Ferre, B. Condon, G. Budahazi, W. Sisson, J.E. Villafranca, C.A. Janson, H.E. McElroy, C.L. Gribskov, et al., Structure of human rhinovirus 3C protease reveals a trypsin-like polypeptide fold, RNA-binding site, and means for cleaving precursor polyprotein, *Cell* 77 (1994) 761–771.
- [7] J. Seipel, A. Guarne, E. Bergmann, M. James, W. Sommergruber, I. Fita, T. Skern, The structures of picornaviral proteinases, *Virus Res.* 62 (1999) 159–168.
- [8] J. Shi, Z. Wei, J. Song, Dissection study on the severe acute respiratory syndrome 3C-like protease reveals the critical role of the extra domain in dimerization of the enzyme: defining the extra domain as a new target for design of highly specific protease inhibitors, *J. Biol. Chem.* 279 (2004) 24765–24773.
- [9] K.V. Holmes, SARS coronavirus: a new challenge for prevention and therapy, *J. Clin. Invest.* 111 (2003) 1605–1609.
- [10] J.E. Blanchard, N.H. Elowe, C. Huitema, P.D. Fortin, J.D. Cechetto, L.D. Eltis, E.D. Brown, High-throughput screening identifies inhibitors of the SARS coronavirus main proteinase, *Chem. Biol.* 11 (2004) 1445–1453.
- [11] C.Y. Wu, J.T. Jan, S.H. Ma, C.J. Kuo, H.F. Juan, Y.S. Cheng, H.H. Hsu, H.C. Huang, D. Wu, A. Brik, F.S. Liang, R.S. Liu, J.M. Fang, S.T. Chen, P.H. Liang, C.H. Wong, Small molecules targeting severe acute respiratory syndrome human coronavirus, *Proc. Natl. Acad. Sci. USA* 101 (2004) 10012–10017.
- [12] U. Bacha, J. Barrila, A. Velazquez-Campoy, S.A. Leavitt, E. Freire, Identification of novel inhibitors of the SARS coronavirus main protease 3CL^{pro}, *Biochemistry* 43 (2004) 4906–4912.
- [13] F. Jean, A. Basak, J. DiMaio, N.G. Seidah, C. Lazure, An internally quenched fluorogenic substrate of prohormone convertase 1 and furin leads to a potent prohormone convertase inhibitor, *Biochem. J.* 307 (Pt. 3) (1995) 689–695.
- [14] W.F. Kuang, Y.C. Lin, F. Jean, Y.W. Huang, C.L. Tai, D.S. Chen, P.J. Chen, L.H. Hwang, Hepatitis C virus NS3 RNA

- helicase activity is modulated by the two domains of NS3 and NS4A, *Biochem. Biophys. Res. Commun.* 317 (2004) 211–217.
- [15] O. Makarova, E. Kamberov, B. Margolis, Generation of deletion and point mutations with one primer in a single cloning step, *Biotechniques* 29 (2000) 970–972.
- [16] C. Huang, P. Wei, K. Fan, Y. Liu, L. Lai, 3C-like proteinase from SARS coronavirus catalyzes substrate hydrolysis by a general base mechanism, *Biochemistry* 43 (2004) 4568–4574.
- [17] K. Fan, L. Ma, X. Han, H. Liang, P. Wei, Y. Liu, L. Lai, The substrate specificity of SARS coronavirus 3C-like proteinase, *Biochem. Biophys. Res. Commun.* 329 (2005) 934–940.
- [18] K. Fan, P. Wei, Q. Feng, S. Chen, C. Huang, L. Ma, B. Lai, J. Pei, Y. Liu, J. Chen, L. Lai, Biosynthesis, purification, and substrate specificity of severe acute respiratory syndrome coronavirus 3C-like proteinase, *J. Biol. Chem.* 279 (2004) 1637–1642.
- [19] S. Chen, L. Chen, J. Tan, J. Chen, L. Du, T. Sun, J. Shen, K. Chen, H. Jiang, X. Shen, Severe acute respiratory syndrome coronavirus 3C-like proteinase N terminus is indispensable for proteolytic activity but not for enzyme dimerization. Biochemical and thermodynamic investigation in conjunction with molecular dynamics simulations, *J. Biol. Chem.* 280 (2005) 164–173.